Carbohydrate Polymers 88 (2012) 609–617

Contents lists available at SciVerse ScienceDirect

Carbohydrate Polymers

journal homepage: www.elsevier.com/locate/carbpol

Equilibrium and kinetics studies on the absorption of Cu(II) from the aqueous phase using a β-cyclodextrin-based adsorbent

Zhanhua Huang[a,*], Shouxin Liu[a], Bin Zhang[a], Lili Xu[b], Xiaofeng Hu[a]

[a] Key Laboratory of Bio-based Material Science and Technology of Ministry of Education, Northeast Forestry University, Harbin 150040, China
[b] Guangzhou Institute of Chemistry CAS, Guangzhou 510650, China

ARTICLE INFO

Article history:
Received 16 August 2011
Received in revised form 14 October 2011
Accepted 3 January 2012
Available online 11 January 2012

Keywords:
β-Cyclodextrin
Adsorbent
Adsorption mechanism
Cu(II)
Kinetics

ABSTRACT

A novel β-cyclodextrin-based adsorbent (CDAA) for the removal of Cu^{2+} was prepared and characterized. The adsorption capacities of Cu^{2+} on CDAA were evaluated under various treatment conditions, including the solution pH, the dosage of the adsorbent, the initial Cu^{2+} concentration, and adsorption time. The results indicated that CDAA hydrogel exhibited typically three-dimensional cross-link network structure. There was a significant increase in the adsorption capacity (from 18.93 mg/g to 107.37 mg/g) when the solution pH increased from 2 to 5. The adsorption equilibrium data were fitted and analyzed with Langmuir, Freundlich, Temkin isotherm equations and four adsorption kinetic models. The results suggested that the Freundlich equation model was the best fit with experimental data ($R^2 = 0.995$). The kinetic equations showed that the adsorption of Cu^{2+} on the adsorbent fit different equations for different concentrations of Cu^{2+}. These results indicate that in the present study, Cu^{2+} adsorption onto the adsorbent occurred via ion exchange and chemical interaction mechanisms.

1. Introduction

Some industrial processes such as electroplating, smelting, sheet metal tooling and mining can produce large quantities of copper-rich wastewater, which would cause serious water pollution. In the environment, the heavy metal copper (Cu) cannot be degraded naturally but accumulates in living organisms through food chain circulation. Although Cu is an essential trace element for most organisms, its excessive accumulation affects the growth and physiological functions of organisms, even causing death. The recommended maximum concentration of Cu^{2+} in drinking water by the World Health Organization is 1.5 mg/L (Liang, Feng, & Guo, 2009).

Cu ion-removal methods from industrial wastewater include chemical precipitation, ion exchange, membrane filtration, electrolysis, solvent extraction, adsorption and biological methods. However, a common disadvantage of the above methods is secondary pollution and low efficiency resulting in high initial and operating costs. In recent years, adsorption resins show great promise for heavy metal ions removal and are increasingly used in wastewater treatments (Jian, Huang, Pang, & Liao, 2008).

β-Cyclodextrin (β-CD) is a cyclic oligosaccharide formed from seven glucose molecules by α-1-4-glucosidic linkages, giving a micro-environment of a chiral, hydrophilic outside and a hydrophobic interior cavity (Balta, Bagdatli, Arsu, Ocal, & Yagci, 2008; Del Valle, 2004). Currently its main uses are in the adsorption of organic chemicals, controlled drug release, environmental protection and cosmetics (Cobos, Cruz, Martinez, Romero, & Casillas, 2008; Guo & Jiang, 2006). Chemical modification of β-cyclodextrin through etherification, esterification and oxidation reactions and cross-linking of hydroxyls outside the interior cavity produce the enhanced adsorption functions on heavy metal ions (Chao, Jin, Xu, Zhuang, & Shen, 2008) as a result of strong interactions between the hydroxyl groups and metal ions. The advantages of β-cyclodextrin and its derivatives as an metal ions adsorbent are the renewable and biodegradable characters; moreover, a large number of active hydroxyl groups can selectively contain and slowly release some substances (Jia, Liu, Fan, & Hu, 2002; Xie & Sun, 2006).

In this paper, the β-cyclodextrin adsorbent, which has a high adsorption capacity for heavy metal ions and water, was synthesized by inverse suspension and redox initiation systems. The possible adsorption mechanisms were also explored using isotherm equations and kinetic models. The present study shows that the β-cyclodextrin adsorbent has high adsorption activities for metal ions in water. The adsorbent can be regenerated and reused and is a potential, excellent multifunctional material for the medical and health fields.

* Corresponding author. Tel.: +86 451 82192905.
E-mail address: huangzh1975@163.com (Z. Huang).

0144-8617/$ – see front matter © 2012 Elsevier Ltd. All rights reserved.
doi:10.1016/j.carbpol.2012.01.009

2. Materials and methods

2.1. Reagents

β-Cyclodextrin (β-CD), acrylic acid (AA), acrylamide (AM), $K_2S_2O_8$, $Cu(NO_3)_2{\cdot}3H_2O$; N,N′-methylene-(bis)-acrylamide (NMBA) were purchased from the chemical reagent development center of Kemiou Engineering, Tianjing, China. A stock solution of Cu(II) (25–150 mg/L) was prepared by dissolution of $Cu(NO_3)_2{\cdot}3H_2O$ with deionized water. Dilute solutions of HNO_3 and NaOH were used for adjusting the initial pH of the solutions.

2.2. Preparation of β-CD based adsorbent, CDAA

β-CD (2.3 g) was first dissolved in NaOH solution and the amount of alkaline solution was controlled to neutralize 75% of the acrylic acid. The alkaline β-CD solution was then placed into a 4-necked round-bottom flask, and 50 mL cyclohexane was added. The mixture was stirred in a water bath under a nitrogen atmosphere. Aqueous solutions of acrylic acid (5.25 g), acrylamide (0.75 g), initiator, and crosslinking agent were poured into two drip funnels under constant pressure to provide the monomer and initiator solution system, respectively. The molar ratio of β-CD, acrylic acid and acrylamide is 0.2:7:1. The reactor was heated to 60 °C under a nitrogen atmosphere, then the monomer and initiator solutions were added to the reactor and reacted for 2–2.5 h. When the reaction was finished, the temperature was maintained at 60 °C for 60 min, and a viscoelastic gel product was obtained. The product was dried under vacuum at 40 °C for 24 h, and then cut into 2 mm × 2 mm × 2 mm cubes.

2.3. Characterization method

The Fourier transform-infrared (FTIR) spectra of the initial β-CD and the CDAA product were recorded with a MAGNA 560 FTIR spectrometer (Thermo Nicolet Corporation, America). A pressed pellet was prepared by grinding the sample powder with IR grade KBr in an agate mortar. The wavelength scan range was 4000–400 cm^{-1} with a resolution of 4 cm^{-1} and an interval of 1.0 cm^{-1}. Solid-state carbon-13 cross-polarization and magnetic-angle spinning nuclear magnetic resonance (^{13}C CPMAS NMR) spectra of the β-CD and CDAA were obtained using a Bruker AVANCE 400 FT-NMR spectrometer with a frequency of 75.47 MHz and a sample spin of 4.0 kHz. The impulse duration at 90° was 4.2 ms, contact time was 1 ms, the number of transients was about 1000, and the decoupling field was 59.5 kHz. Chemical shifts were determined relative to tetramethyl silane (TMS). The spectra were accurate to 1 ppm. The spectra were run without suppression of spinning side bands. Scanning electron microscope (SEM) was taken with a FEI QUANTA 200 microscope. The hydrogels swollen to equilibrium in the Cu^{2+} concentrations of 100 mg/L at 37 °C for 24 h were frozen in liquid nitrogen and snapped immediately, and then freeze-dried. The fracture surface (cross-section) of the hydrogel was observed and photographed.

2.4. Batch adsorption experiments

The $Cu(NO_3)_2{\cdot}3H_2O$ was firstly dissolved into deionized water and then diluted to the required concentration after the pH was adjusted using HNO_3 or NaOH. A certain amount of the prepared adsorbent was added to solutions containing various concentrations of Cu^{2+} ions. The ions were allowed to adsorb at room temperature for 24 h, before the solution was filtered. The concentration of the Cu^{2+} ions in the filtrate was measured by atomic absorption spectrophotometer. The adsorption capacity (Q) and removal rate (A) were calculated as follows:

$$Q = \frac{C_0V_0 - C_eV_e}{C_0V_0} \times 100\% \quad (1)$$

$$A = \frac{C_0V_0 - C_eV_e}{m} \quad (2)$$

where C_0 and C_e are the initial and equilibrium concentrations of Cu^{2+}, respectively; V_0 and V_e are the initial and equilibrium volumes of the solution, respectively; and m is the mass of the CDAA used.

To determine the adsorption kinetics and adsorption isotherms, 100 mL of the Cu^{2+} solution (equivalent to either 25 mg/L, 50 mg/L, 100 mg/L or 150 mg/L), was added to 0.09 g of the CDAA. The temperature was maintained at 25 °C and the solution was shaken for 240 min. At various intervals, the adsorbent and the solution were separated by filtration and the adsorbent was weighted. The solution phase was diluted and the Cu^{2+}concentration in the solution was measured. The effects of the amount of adsorbent, the pH, and the initial Cu^{2+} concentration on the adsorption capacity were systematically investigated.

3. Results and discussion

3.1. Characterization of CDAA

The FTIR spectra of β-CD and CDAA are shown in Fig. 1. The stretching vibration absorption peak of –OH group is around 3400 cm^{-1} and the peak for C–H at 2900 cm^{-1}, while the stretching vibration peak for the carboxylic acid –C=O is 1600–1700 cm^{-1}, and the bending vibration peak for C–H is near 1450 cm^{-1}. Comparing the FTIR spectra for β-CD and CDAA, it is clear that the –OH peak for β-CD at 3404 cm^{-1} is strong and wide, while for the CDAA resin the peak has moved to a lower wave number with a strong and broad absorption peak 3363 cm^{-1}. Also, due to increasing hydrogen bonding between molecules, the hydroxyl group absorption peak has broadened for CDAA. The peak at 1157 cm^{-1} is attributed to the stretching vibration of the C–O–C bond on β-CD and CDAA. Another two absorption peaks near 1108 cm^{-1} and 1030 cm^{-1} are characteristic of the primary and secondary alcohol groups on β-CD (Bai, Wang, Wang, Ma, & Ni, 2006; Xie, Chen, Liu, & Xu, 2007). The $-CH_2$ stretching vibrations at 2925 cm^{-1} and 2846 cm^{-1} increased significantly in CDAA, possibly due to the formation of $-CH_2$ in the polymerization process during the introduction of the acrylic acid and acrylamide monomer. The strong, overlapping peaks occurring at 1671 cm^{-1} can be attributed to the –C=O stretching vibration peaks in acid amides and carboxylic acids (Kuang, YuK, & Huh, 2011). The strong stretching vibration peak at 1570 cm^{-1} is the N-H

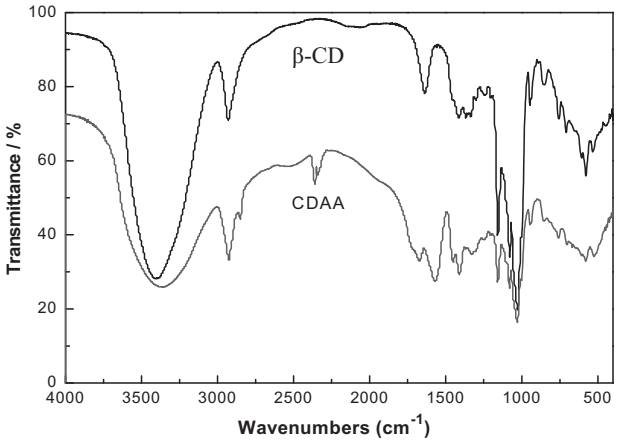

Fig. 1. FTIR spectra of the β-CD and CDAA.

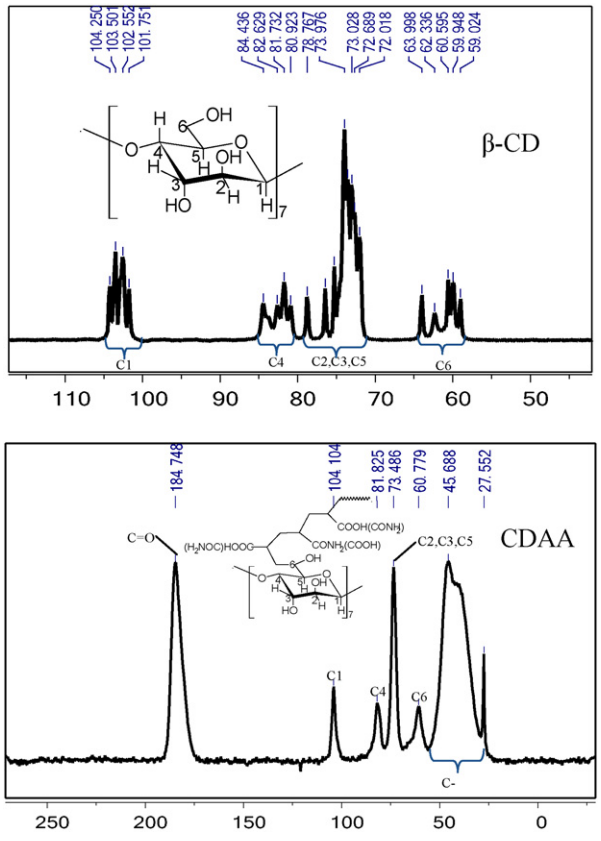

Fig. 2. Solid-state ^{13}C NMR spectra of the β-CD and CDAA.

absorption peak in an acylamino group on CDAA. The asymmetric stretching vibration of the sodium carbonyl group of –COONa in sodium polyacrylate is seen in the peak at 1451 cm^{-1}, while the strong band at 1410 cm^{-1} is either a stretching vibration peak for C–N or a bending vibration peak for $–CH_2–$, indicating the presence of acylamino groups on the CDAA. Based on these results, we can conclude that carboxyl and amide groups have been introduced to the CDAA product; the lack of a characteristic –C=C absorption peak indicates a polymerization reaction between β-CD, acrylic acid and acrylamide.

The chemical structures of the β-CD and CDAA were confirmed by solid-state NMR spectroscopy (^{13}C NMR) (Fig. 2). The NMR spectrum shows a asymmetric β-CD cavity as indicated by the clear signal separation of the characteristic carbon atoms. The peaks at 101–104 ppm are the C1 signal peaks connected to the β-CD vertical glycosidic linkage. The chemical shift at 80–84 ppm reflect the characteristic signals for C4; the separated peaks at 59–64 ppm are characteristic of the signal for C6, and the chemical shift at 72–78 ppm represent the cyclic carbons C2, C3, C5 that are not connected with the glycosidic bond, but have the same characteristics as the separated peaks.

The β-CD polymerization to form CDAA resulted in the distorted separation signals of the corresponding NMR spectra, while the signals for the other carbon atoms became smooth. The characteristic peak at 184.75 ppm represented carbon signal from C=O; the other three peaks at 104.10 ppm, 81.82 ppm and 60.78 ppm represented C1, C4 and C6 signals of the glucose residues, respectively. The peak at 73.49 ppm was identified as the cyclic carbons C2, C3 and C5, which are not connected with the glycosidic linkage; in certain environments, the resonance peaks of C2, C3, C5 tend to overlap to form a single peak (Lu, Yang, Zhou, & Lei, 2008). The peaks at 20–60 ppm are characteristic signal peaks from different forms of the polymerase chains (Oo, Kassim, & Pizzi, 2009). The above results demonstrated the polymerization conversion of residual β-CD to CDAA (Wan, 2008).

3.2. Morphology investigation

Fig. 3 shows the SEM images of the cross-sections of the freeze-dried CDAA hydrogels samples in various Cu^{2+} concentrations. CDAA hydrogel exhibited typically macropores texture. Moreover, the size of the three-dimensional network structure decreased with the increase of Cu^{2+} concentration, leading to a more compact of macropores. This implies the competitive adsorption on CDAA surface between the $Cu^{2+}$and H_2O. Moreover, complexation of the Cu^{2+} and CDAA can reduce the space in the networks of hydrogels; this is helpful for the diffusion of numerous water molecules into CDAA, leading to the higher swelling ratio. Therefore, the size of three-dimensional network of the hydrogels was widen, with the decrease in the Cu^{2+}concentration.

3.3. Adsorption studies

3.3.1. Effects of adsorbent dosage

As shown in Fig. 4, the removal rate of Cu^{2+} was highest at the CDAA dose of 0.09 g. The removal rate showed a smooth downward trend with the increase in CDAA dosage. In contrast, the adsorption capacity gradually decreased with the increasing adsorbent dosage. A possible reason for this reduction may be that the added adsorbent provided excessive active groups beyond the capacity to be accepted by the metal ions; in addition to that, due to the competition for active groups on the adsorbent between water and metal ions, an increase in water adsorption capacity would result in a decrease in the removal capacity of the metal ions. Considering the two factors (adsorption capacity and removal rate), it can be concluded that the optimal CDAA dose is 0.09 g for the maximum removal of Cu^{2+} from solutions of 100 mg/L.

3.3.2. Effect of pH on Cu^{2+} uptake by CDAA

The pH of solution has an important influence on the adsorption capacity (Fig. 5). The adsorption capacity of the prepared CDAA to Cu^{2+} was 18.93 mg/g at the solution of pH 2. The adsorption capacity was increased significantly with the increase in solution pH from 2 to 5. This may be due to the fact that at lower solution pH values, H^+ competes with metal ions for adsorption sites, resulting in the surface of the adsorbent occupied by more H^+, thus reducing the complexation of metal ions on the surface of the adsorbent (Liang, Guo, Feng, & Tian, 2010). At higher pH values, the surface of adsorbent is occupied by more negative charges, attracting more metal ions. When the pH value increased to 5.5 and 6 or higher, the complexation of negative hydroxide ions occurs, which means the Cu^{2+} will produce a flocculated precipitate, from which the adsorption data cannot be measured.

3.3.3. Effect of initial Cu^{2+} concentration

The initial Cu^{2+} concentration in the solution also influences the adsorption capability of the CDAA adsorbent. 0.05 g CDAA was added in solution of Cu^{2+} with concentration of 25 mg/L, 50 mg/L, 100 mg/L and 150 mg/L, respectively. So that the amount of Cu^{2+} ions in the residual solution could be measured and the adsorption capacity and removal rate could be calculated. The results showed that the adsorption capacity increases with the increasing Cu^{2+} concentration, and the removal rate is highest when the Cu^{2+}concentration is 100 mg/L (Fig. 6). As the concentration of Cu^{2+} ions increases, more and more metal ions combine with the active groups on the resin, which is seen in the gradual increase in the adsorption capacity. However, when the concentration of Cu^{2+} ions becomes higher, the increasing trend in metal ions combining with

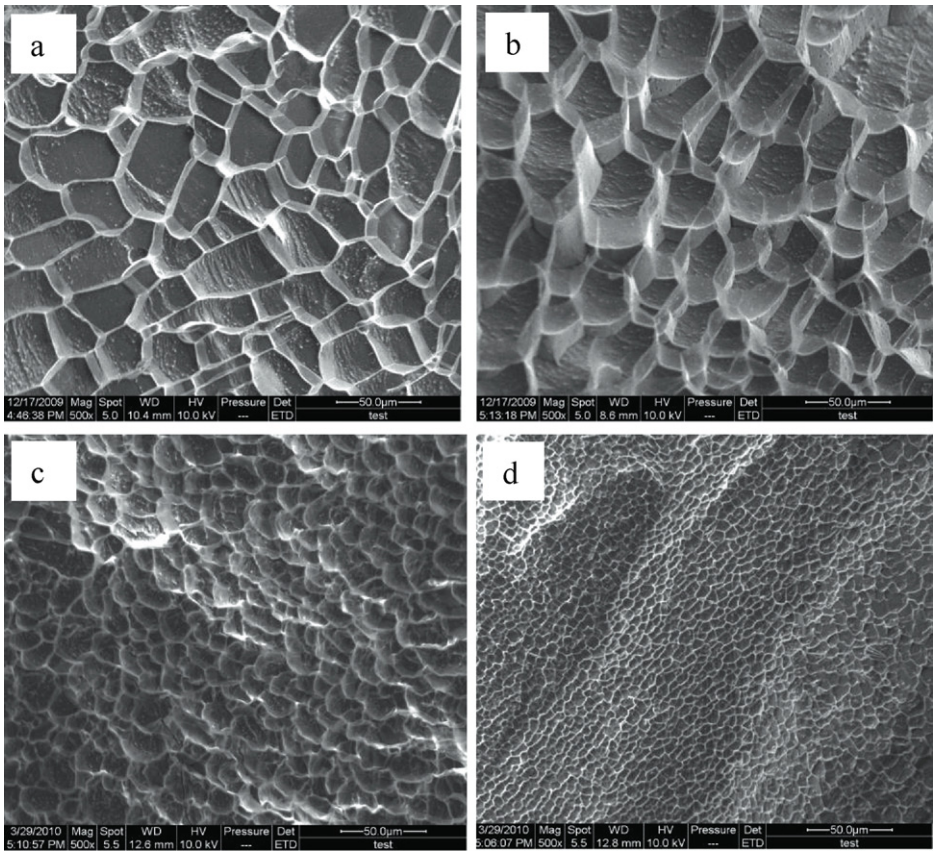

Fig. 3. SEM images of CDAA hydrogels in (a) distilled water, (b) 25 mg/L Cu^{2+}, (c) 50 mg/L Cu^{2+} and (d) 100 mg/L Cu^{2+}.

the active groups becomes slower. Therefore, within the experimental range, the removal rate increases initially, then decreases. Combining the changes in adsorption capacity and removal rate, it can be concluded that when the amount of the adsorbent in 0.05 g, the greatest adsorption effect is seen when the concentration of Cu^{2+} ions is 100 mg/L.

3.3.4. *Effect of adsorption time*

The adsorption time is a very important factor affecting the adsorption of metal ions onto resins. The experiments were conducted at room temperature, with 0.09 g of CDAA and Cu^{2+} concentrations of 25 mg/L, 50 mg/L, 100 mg/L and 150 mg/L. The adsorption capacities of CDAA for Cu^{2+} after various adsorption durations are shown in Fig. 7. The adsorption capacity of CDAA for Cu^{2+} at different concentrations increases with the increase of contact time, but it does not fit a linear relationship. Based on the adsorption curve, the adsorption of Cu^{2+} onto CDAA can be divided into two phases: the rapid adsorption stage – the adsorption of Cu^{2+} onto the outer surface of CDAA; the slow adsorption stage – progressive adsorption. Because there are a large number of active sites on the surface of the CDAA resin, during the initial phase the concentration difference causes a fast mass transfer, and the Cu^{2+} is easily adsorbed by the resin (Jiang, Zhao, Wei, Zhu, & Ni, 2008; Sengil & Özacar, 2009; Sengil, Özacar, & Türkmenler, 2009). As the adsorption time increases, the accumulation of Cu^{2+} on the CDAA reduces the number of active adsorption sites available, hindering the further transfer of Cu^{2+} and resulting in nonlinear absorption (Kennedy, Vijaya, Sekaran, & Kayalvizhi, 2007). It can be seen from the Fig. 4 that when the Cu^{2+} concentration is 25 mg/L, the maximum adsorption is achieved with an adsorption time of 30 min. The adsorption capacity did not increase with further adsorption time, so it can be concluded that the adsorption equilibrium required for 30 min in a 25 mg/L Cu^{2+} solution. When the Cu^{2+} concentration is 50 mg/L, the adsorption equilibrium required for 90 min, the maximum adsorption capacity was 36.28 mg/g. For Cu^{2+} concentrations of 100 mg/L and 150 mg/L, the adsorption equilibrium required for more than 180 min. In summary, at lower Cu^{2+} concentrations, adsorption equilibrium is achieved faster, the equilibrium time extends with the increase in the Cu^{2+} concentration.

The initial Cu^{2+} concentration provides a driving force to overcome the mass transfer resistance between the liquid and solid, increasing the probability of collisions between the surfaces of the Cu^{2+} and the adsorbent (Ngah & Hanafiah, 2008), thus increasing the absorption capacity and reducing the Cu^{2+} concentration in the residual solution. When the contact time is longer than the equilibrium time, the concentration of Cu^{2+} in the residual solution maintains unchanging. It implies no change of the adsorption capacity (Q).

3.4. *Results of equilibrium experiments*

The equilibrium experiments were carried out for the adsorption of Cu^{2+} by CDAA. Adsorption isotherms are basic requirements for the understanding of a sorption system, and it is important to establish the most appropriate correlation for each equilibrium curve. The distribution of metal ions between the liquid phase and the adsorbent is a measure of the equilibrium point during the adsorption process, and it can be expressed by various isotherm models. In this study, three isotherm equations viz. the Langmuir, Freundlich and Temkin isotherms were used to evaluate the adsorption process. Linear regression analysis was used to evaluate the fit of various isotherms to the experimental equilibrium data.

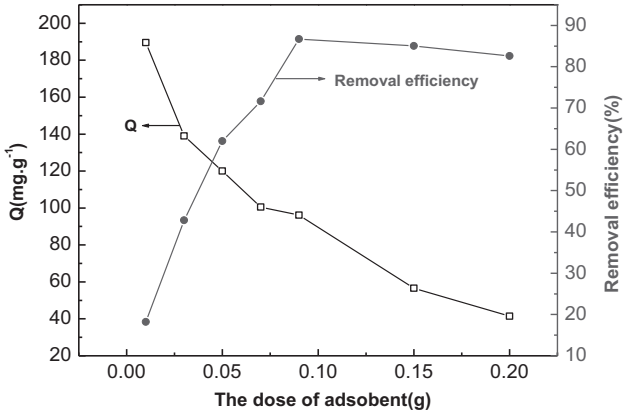

Fig. 4. Effect of the dose of adsorbent, CDAA, on adsorption of Cu^{2+} (100 mg/L concentration, 100 μm particle size, contact time 240 min, 298 K temperature, pH 3.6 and stirring speed 120 rpm).

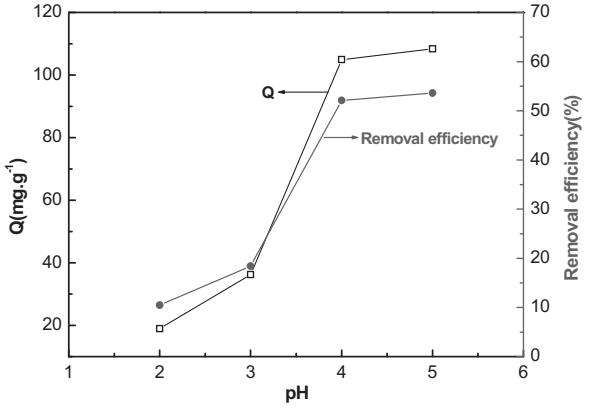

Fig. 5. Effect of pH on absorption of Cu^{2+} by CDAA (100 mg/L concentration, 298 K temperature and 0.09 g CDAA, contact time 240 min, 100 μm particle size, stirring speed 120 rpm).

3.4.1. Langmuir isotherm

The Langmuir isotherm describes a monolayer adsorption process, which is based on the assumption that all the adsorption sites are equivalent and adsorption to the active sites is independent of the adjacent sites. The Langmuir isotherm model (Langmuir, 1918; Ogata & Nakano, 2005) is described by the equation:

$$q_e = K_L \frac{C_e}{(1 + a_L C_e)} \tag{3}$$

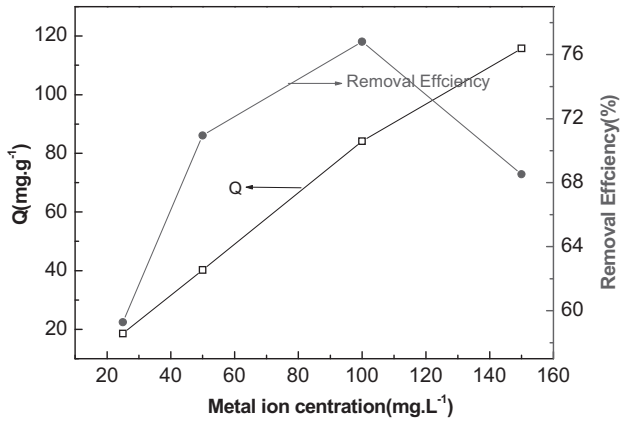

Fig. 6. Influence of initial Cu^{2+}concentration on absorption by CDAA (298 K temperature, 0.05 g CDAA, contact time 240 min, 100 μm particle size, stirring speed 120 rpm).

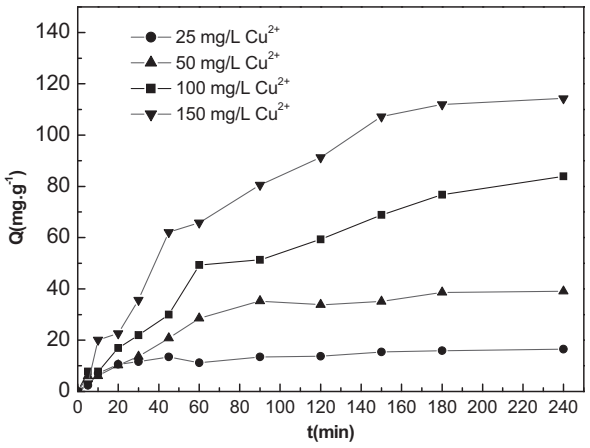

Fig. 7. Influence of contact time on the absorption of Cu^{2+}.

where q_e (mg/g) and C_e (mg/L) are the amount of Cu^{2+} adsorbed per unit weight of adsorbent and the unadsorbed Cu^{2+} concentration in solution at equilibrium, respectively. The empirical constants K_L and a_L for Langmuir model are related to the maximum adsorptive capacity of the adsorbent (L/g) and the bonding strength (L/mg), respectively.

3.4.2. Freundlich isotherm

The Freundlich isotherm describes a monomolecular coverage layer of the adsorbent by the solutes (Al-Asheh, Banat, Al-Omari, & Duvnjak, 2000). It is an empirical isotherm model used for adsorption onto heterogeneous surfaces or surfaces which support sites of varying affinities (Dabrowski, 2001). The Freundlich isotherm model is described by the following equation:

$$\log\ q_e = \log K_F + \frac{1}{n} \log C_e \tag{4}$$

where q_e is the amount adsorbed at equilibrium (mg/g); C_e is the equilibrium concentration of Cu^{2+} (mg/L); and K_F (mg/g) and n (g/L) are Freundlich constants related to the adsorption capacity and the intensity of adsorption, respectively.

3.4.3. Temkin isotherm

The Temkin isotherm is another empirical model for studying the adsorption process. Temkin considered that during the sorbate to adsorbent interactions, the heat of adsorption of all the molecules in the layer would decrease linearly with coverage (Tempkin & Pyzhev, 1940). The Temkin isotherm equation is given below:

$$q_e = B\ \ln A + B \ln C_e \tag{5}$$

where q_e (mg/g) is the amount of adsorbed Cu^{2+} per unit weight of adsorbent; C_e (mg/L) is the concentration of unadsorbed Cu^{2+} in solution at equilibrium; and A and B are the Temkin constants.

The isotherm constants were determined from linear isotherm graphs for each of the isotherm equations tested. The values of the isotherm constants and the correlation coefficients in the Cu^{2+}–CDAA system are shown in Table 1. In the present study, high R^2 value indicated that the isotherm best fits the adsorption equilibrium data. The Freundlich isotherm provided R^2 value (0.995) slightly higher than that obtained with the Langmuir model (0.913) and Temkin model (0.936). The Freundlich equation model was best fit for the experimental data. The results indicates that the CDAA surface is heterogeneity in nature and this surface is heterogeneity is another factor favoring Cu^{2+} adsorption on CDAA and for a highly heterogeneity system. So, the Freundlich equation model was better than the Langmiur and Temkin isotherm equations (Anirudhan, Jalajamony, & Suchithra, 2009; Tseng et al., 2009).

Table 1
Langmuir, Freundlich and Temkin isotherm constants for the adsorption of Cu^{2+} onto CDAA.

Langmuir				Freundlich			Temkin		
K_L (L/g)	α_L (L/mg)	Q_0 (mg/g)	r^2	K_F (L/g)	n	r^2	B	A (L/g)	r^2
30.13	0.268	112.41	0.913	8.074	3.28	0.995	7.12	1.364	0.936

Theoretically, the maximum adsorption capacity of Cu^{2+} was 112.41 mg/g, close to the actual maximum adsorption capacity (107.37 mg/g) measured.

3.5. Adsorption kinetics

The influences of adsorption time and initial solution concentration on adsorption capacity are shown in Fig. 7. Results showed that a higher initial Cu^{2+}concentration results in a larger initial adsorption rate. To analyze the mechanism of the adsorption process, a quasi-first-order adsorption rate equation, a quasi-second-order adsorption rate equation, the Elovich equation and the particle diffusion equation were tested to fit the adsorption curve.

3.5.1. Fit using the quasi-first-order kinetic model

The quasi-first-order kinetic equation is also known as the quasi-first-order rate equation or the Lagergren quasi-first-order kinetic equation. This model is based on the assumption that the adsorption rate is determined by the number of adsorption sites on the surface of the adsorbent (Bai et al., 2006). The equation is as follows:

$$\log(Q_{e,1} - Q_t) = \log\ Q_{e,1} - \frac{K_1}{2.303}t \tag{6}$$

where Q_t and $Q_{e,1}$ represents the amount of Cu^{2+} at time, t and at equilibrium, respectively and K_1 is the adsorption equilibrium constant for the adsorption process.

Fig. 8(a) shows the quasi first-order equation based on the experimental data shown in Fig. 7. The coefficients for the equation, the values for $\log(Q_{e,1} - Q_t)$, and the correlation coefficients are listed in Table 2. The equilibrium adsorption capacity of the CDAA increased with the increasing Cu^{2+} concentration. The R^2 values for the quasi-first-order kinetic equations fitted for different Cu^{2+} concentrations are all greater than 0.88 with no regular variation. Therefore, the adsorption of Cu^{2+} onto CDAA does not meet the quasi-first-order kinetic equation (Liu, Yao, Zhou, Xu, & Wei, 2009).

3.5.2. Fit using the quasi-second-order kinetics model

The quasi-second-order kinetic model is based on the assumption that the adsorption rate is determined by the square of the number of vacant adsorption sites on the surface of adsorbent (Xie et al., 2007). The equation is shown as follows:

$$\frac{t}{Q_t} = \frac{1}{K_2 Q_{e,2}^2} + \frac{1}{Q_{e,2}}t \tag{7}$$

where K_2 is the equilibrium constant of the quasi-second-order equation (g/mg min). Fig. 8(b) shows the experimental data from Fig. 7 fitted to a quasi-second-order curve showing the adsorption of Cu^{2+} onto CDAA at time t. The coefficient and correlation values for the equations are listed in Table 2.

The results in Table 2 indicate that the equilibrium adsorption capacity of CDAA increased gradually with increasing Cu^{2+} concentrations. The R^2 values, depending on the concentrations of Cu^{2+}, ranged from 0.92 to 0.98, indicating that the adsorption process is in line with a quasi-second-order kinetics model. At low Cu^{2+} concentrations (25 mg/L, 50 mg/L), the quasi-second-order kinetic equations have R^2 values of 0.988 and 0.963, respectively, with only a small difference; it indicates that the adsorption process is affected by ion-exchange, or there is complexation between the Cu^{2+} and the surface of the adsorbent (Renault, Morin-Crini, Gimbert, Badot, & Crini, 2008).

In most cases, the first-order Lagergren equation can only be used for the initial stage of the adsorption process rather than the whole process, while the quasi-second-order kinetic model assumes that the rate-limiting step may be chemical adsorption, and is used in many adsorption studies (Kumar, King, & Prasad, 2006). From the analysis above, we can conclude that the adsorption capacity of CDAA at low Cu^{2+} concentrations (25 mg/L, 50 mg/L) changes with time and the adsorption curve was fitted well by the quasi-second-order kinetic equation.

3.5.3. Fit using the Elovich equation

The quasi-first-order and quasi-second-order kinetic models described above cannot determine the diffusion mechanism of Cu^{2+} onto the CDAA resins. The Elovich equation and the intraparticle diffusion equation are needed to fit the experimental data from Fig. 7 to consider the diffusion mechanisms. The Elovich equation is as follows:

$$Q_t = \frac{1}{\beta}\ln(\alpha\beta) + \frac{1}{\beta}\ln t \tag{8}$$

Table 2
Kinetic parameters for the adsorption of CDAA at different initial Cu^{2+} concentrations.

Kinetics	Parameters	Cu^{2+}, C_0 (mg/L)			
		25	50	100	150
Pseudo-first-order	$Q_{e,exp}$ (mg/g)	16.54	39.08	83.89	114.29
	K_1 (min^{-1})	0.01250	0.01421	0.02135	0.01989
	$Q_{e,cal}$ (mg/g)	87.8456	9.97103	42.69431	141.7849
	R^2	0.96458	0.88572	0.89766	0.94201
Pseudo-second-order	K_2 (min^{-1})	0.00254	0.00032	0.00621	8.50442E−05
	$Q_{e,cal}$ (mg/g)	17.6616	50.47956	12.73885	153.6098
	R^2	0.98829	0.96353	0.92131	0.93443
Elovich	K_1 (min^{-1})	0.01250	0.01421	0.02135	0.01989
	$Q_{e,cal}$ (mg/g)	87.8456	9.97103	42.69431	141.7849
	R^2	0.91061	0.91196	0.92332	0.95983
Intraparticle diffusion	K_{int} (mg/g $min^{1/2}$)	4.93424	0.21025	−8.97196	−9.36187
	R^2	0.77790	0.90979	0.97907	0.96146

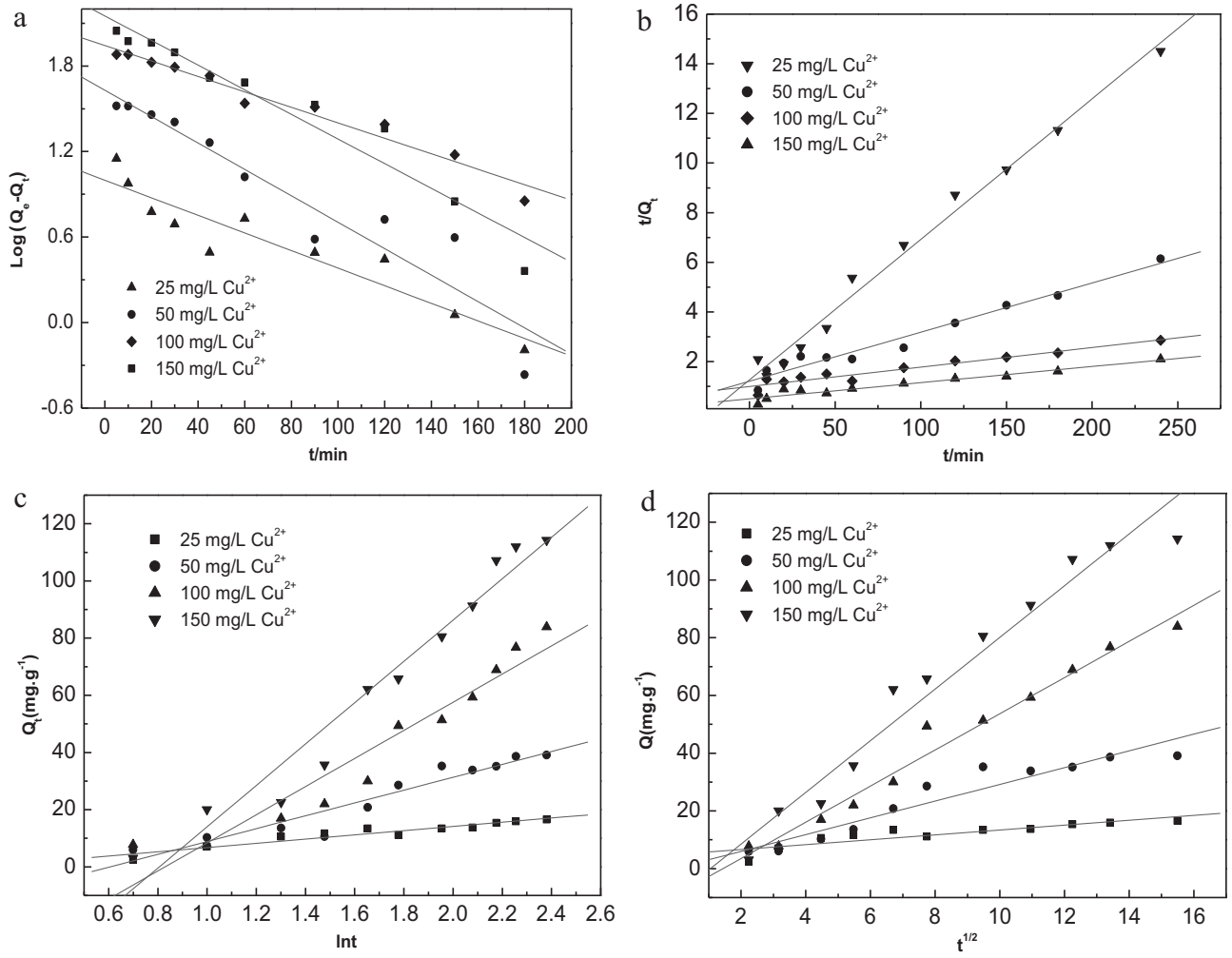

Fig. 8. Plots of the (a) pseudo-first-order equation, (b) pseudo-second-order equation, (c) Elovich equation and (d) intraparticle diffusion equation for the adsorption kinetics of Cu^{2+} on CDAA at different initial concentrations.

where α is the initial adsorption constant (mg/g min^{-1}); and β is a coefficient related to the surface coverage and the activation energy for the chemical adsorption (g/mg). Fig. 8(c) shows the linear fit of the Elovich equation model when the CDAA resin adsorbs different concentrations of Cu^{2+}. The coefficient, β, and correlation values for the Elovich equation are listed in Table 2.

Table 2 shows that at equilibrium situation, the adsorption capacity of the CDAA resin for Cu^{2+} ($Q_{e,cal}$) gradually increases with the increase in Cu^{2+} concentration, and the corresponding correlation coefficient values for the Elovich equation also show a gradually increasing trend, from 0.91 for a Cu^{2+} concentration of 25 mg/L to 0.959 when the Cu^{2+} concentration is 150 mg/L. Thus, for higher initial Cu^{2+}concentrations, the chemical activation energy is higher and there is more chemical adsorption, giving a trend of gradually increasing values for $Q_{e,cal}$. These results indicate that the adsorption of Cu^{2+} onto CDAA at higher concentrations is more consistent with the Elovich equation.

3.5.4. Fit using the intraparticle diffusion model

The intraparticle diffusion equation is based on the model proposed by Weber and Morris, also known as Weber–Morris equation, which is shown as follows:

$$O_t = K_{int} t^{1/2} + C \quad (9)$$

where K_{int} is the constant for the particle diffusion rate (mg/g $min^{1/2}$); and C characterizes the extent of the boundary layer effect. Fig. 8(d) fits values of Q_t to $t^{1/2}$, and if the curve passes through the origin (0, 0), intraparticle diffusion can be considered as the rate-limiting step, otherwise, the adsorption process is jointly controlled by a variety of adsorption mechanisms (Tan, Ahmad, & Hameed, 2009).

The Weber–Morris equation has been used to fit the experimental data from Fig. 7 and obtain linear forms of the diffusion model for the adsorption of Cu^{2+} at different concentrations to the CDAA resin, with the results shown in Fig. 8(d). The results of fitting do not pass through the origin (0, 0) indicating that particle diffusion is not the only rate-limited step in the adsorption process (Acharya, Sahu, Mohanty, & Meikap, 2009). The coefficients and numerical values from the equation are listed in Table 2. The correlation coefficient, R^2, for the adsorption of Cu^{2+} is as high as 0.979. As the initial Cu^{2+} concentration increased, the R^2 value also increased gradually, which is probably due to the porous structure of the CDAA, so that high Cu^{2+} concentrations can lead to diffusion among the particles. Therefore, for high solution Cu^{2+} concentrations, the adsorption process proceeded with stronger intraparticle diffusion (Acharya et al., 2009).

3.6. Adsorption mechanism

The process of metal ion adsorption can be divided into three stages: transmission of ions to the surface of adsorbent from solution; adsorption of the ions onto the surface of the adsorbent;

and the diffusion of the ions into the adsorbent. In the adsorption process, initial adsorption rate is faster, this may be due to the higher concentration of the ions and the more adsorption sites available on the surface of adsorbent is beneficial to the ions adsorption onto the surface of adsorbent. During the subsequent stages, because the adsorption rate is largely related to diffusion of the ions within the adsorbent, the adsorption rate is slower.

For Cu^{2+} adsorption at low concentrations, there are more adsorption sites available, and although chemical adsorption occurs, ion exchange processes are more likely as seen from the R^2 values obtained with the quasi-second-order kinetic equation, which are in the range of 0.963 to 0.988.

At the higher Cu^{2+} concentration (100 mg/L, 150 mg/L), the adsorption behavior fitted both the Elovich kinetic equation and the intraparticle diffusion equation well. The results show that the higher initial Cu^{2+} concentrations, the stronger diffusion driving forces are; which in turn, a lower initial concentration is more conducive to processes of chemical adsorption and intraparticle diffusion. Although ion exchange has an effect on adsorption at higher Cu^{2+} concentrations, complexation between Cu^{2+} and the surface of adsorbent is dominant, which is also confirmed by the higher R^2 values for the Elovich and intraparticle diffusion models. CDAA contains six adjacent hydroxyl groups for binding metal ions. The mechanism of metal ions adsorption onto the different phenolic compounds in the resin is a matter of considerable debate. The suggested mechanisms include ion exchange, surface adsorption, chemisorption, complexation, and adsorption-complexation (Ren, Zhang, & Zhao, 2008; Zhao et al., 2010). This study indicates that the adsorption mechanism may be partly the result of ion exchange or chemical adsorption between the Cu^{2+} ions and the hydroxyl groups on the CDAA surface. The adsorption at lower pH values decreases due to the ion exchange equilibrium as H^+ ions are released during the ion exchange process. Therefore, at lower pH values, the ion exchange equilibrium moves to the left.

4. Conclusions

A copolymer resin, CDAA, formed from β-cyclodextrin, acrylic acid (AA) and acrylamide (AM) can be used to remove Cu^{2+} from wastewater. CDAA hydrogel exhibited typically three-dimensional cross-link network structure. The adsorption of Cu^{2+} on CDAA is increase with the increase of pH and ionic strength. The maximum adsorption capacity is as high as 107.37 mg/g at a Cu^{2+} concentration of 80 mg/L. The kinetic model results indicate that adsorption of Cu^{2+} onto the CDAA fit the quasi-second-order and Elovich equations well at a low Cu^{2+} concentrations (25 mg/L, 50 mg/L), and the two models provide the best correlation for the biosorption process. The intraparticle diffusion model also fits the experimental data well at high Cu^{2+} concentrations (100 mg/L, 150 mg/L). The adsorption mechanism may be partly the result of ion exchange or chemical interactions between the Cu^{2+} ions and hydroxyl groups on the CDAA surface.

Acknowledgments

This work was supported financially by the National Natural Science Foundation of China (no. 31000277) and the Central University Basic Scientific Research Project of China (no. DL11EB01). We also thank the PhD Programs Foundation of Ministry of Education of China (no. 20100062120005) and Natural Science Foundation of Heilongjiang Province of China (no.C201033).

References

Acharya, J., Sahu, J. N., Mohanty, C. R., & Meikap, B. C. (2009). Removal of lead(II) from wastewater by activated carbon developed from Tamarind wood by zinc chloride activation. *Chemical Engineering Journal*, *149*, 249–262.

Al-Asheh, S., Banat, F., Al-Omari, R., & Duvnjak, Z. (2000). Prediction of binary sorption isotherms for the sorption of heavy metals by pine bark using single isotherm data. *Chemosphere*, *41*, 659–665.

Anirudhan, T. S., Jalajamony, S., & Suchithra, P. S. (2009). Improved performance of a cellulose-based anion exchanger with tertiary amine functionality for the adsorption of chromium(VI) from aqueous solutions. *Colloid and Surfaces A: Physicochemical and Engineering Aspects*, *335*, 107–113.

Bai, J., Wang, R. W., Wang, J. X., Ma, G. H., & Ni, W. (2006). Immobilization and characterization of β-cyclodextrin on polyglycidylmethacrylate porous microspheres. *Ion Exchange and Adsorption*, *22*, 97–104.

Balta, D. K, Bagdatli, E., Arsu, N., Ocal, N., & Yagci, Y. (2008). *Journal of Photochemistry and Photobiology A*, *196*, 33–37.

Chao, Y., Jin, Z. Y., Xu, X. M., Zhuang, H. N., & Shen, W. Y. (2008). Preparation and stability of the inclusion complex of astaxanthin with hydroxypropyl-β-cyclodextrin. *Food Chemistry*, *109*, 264–268.

Cobos, L. A., Cruz, C. A., Martinez, H. A., Romero, M., & Casillas, G. (2008). Synthesis of magnetite nanoparticles–β-cyclodextrin complex. *Journal of Alloys and Compounds*, *466*, 330–334.

Dabrowski, A. (2001). Adorption – From theory to practice. *Advances in Colloid and Interface Science*, *93*, 135–224.

Del Valle, E. M. (2004). Cyclodextrins and their uses: A review. *Process Biochemistry*, *39*, 1033–1046.

Guo, M. Y., & Jiang, M. (2006). Macromolecular self-assembly based on inclusion complexation of cyclodextrins. *Progress in Chemistry*, *19*, 557–566.

Jia, J. F., Liu, Q., Fan, X. D., & Hu, H. (2002). Swelling behavior of interpenetrating hydrogel networks based on a thermosensitive PUE-β-CD/PNIPAM polymer. *Journal of Functional Polymers*, *15*, 281–285.

Jian, Y., Huang, C. J., Pang, H., & Liao, B. (2008). Progress in cellulose-based adsorbents. *Chemistry*, *12*, 891–899.

Jiang, X., Zhao, J. P., Wei, F., Zhu, C. P., & Ni, C. H. (2008). Synthesis and adsorption properties of crosslinked polyacrylamide modified by thiosemicarbazide. *Journal of Jiangnan University (Natural Science Edition)*, *7*, 350–353.

Kennedy, L. J., Vijaya, J., Sekaran, G., & Kayalvizhi, K. (2007). Equilibrium, kinetic and thermodynamic studies on the adsorption of *m*-cresol onto micro- and mesoporous carbon. *Journal of Hazardous Materials*, *149*, 134–143.

Kuang, J., YuK, K. Y., & Huh, K. M. (2011). Polysaccharide-based superporous hydrogels with fast swelling and superabsorbent properties. *Carbohydrate Polymers*, *83*, 284–290.

Kumar, Y. P., King, P., & Prasad, V. S. R. K. (2006). Equilibrium and kinetic studies for the biosorption system of copper(II) ion from aqueous solution using *Tectona grandis* L.f. leaves powder. *Journal of Hazardous Materials*, *137*, 1211–1217.

Langmuir, I. (1918). The adsorption of gases on plane surface of glass, mica and platinum. *Journal of the American Chemical Society*, 1361–1368.

Liang, S., Feng, N. C., & Guo, X. Y. (2009). Progress of heavy metal wastewater treatment by biosorption. *Technology of Water Treatment*, *35*, 13–17.

Liang, S., Guo, X. Y., Feng, N. C., & Tian, Q. C. (2010). Isotherms, kinetics and thermodynamic studies of adsorption of Cu^{2+} from aqueous solutions by Mg^{2+}/K^+ type orange peel adsorbents. *Journal of Hazardous Materials*, *174*, 756–762.

Liu, B. Y., Yao, Z., Zhou, Z., Xu, H., & Wei, P. (2009). Kinetics and thermodynamics of the adsorption of copper(II) onto chelating resin. *The Chinese Journal of Process Engineering*, *9*, 865–870.

Lu, D. D., Yang, L. Q., Zhou, T. H., & Lei, Z. Q. (2008). Synthesis, characterization and properties of biodegradable polylactic acid-β-cyclodextrin cross-linked copolymer microgels. *European Polymer Journal*, *44*, 2140–2145.

Ngah, W. S. W., & Hanafiah, M. A. K. (2008). Adsorption of copper on rubber (*Hevea brasiliensis*) leaf powder: Kinetic, equilibrium and thermodynamic studies. *Biochemical Engineering Journal*, *39*, 521–530.

Ogata, T., & Nakano, Y. (2005). Mechanisms of gold recovery from aqueous solutions using a novel tannin gel adsorbent synthesized from natural condensed tannin. *Water Research*, *39*, 4281–4286.

Oo, C. W., Kassim, M. J., & Pizzi, A. (2009). Characterization and performance of *Rhizophora apiculata* mangrove polyflavonoid tannins in the adsorption of copper(II) and lead(II). *Industrial Crops and Products*, *30*, 152–161.

Ren, Y. M., Zhang, M. L., & Zhao, D. (2008). Synthesis and properties of magnetic Cu(II) ion imprinted composite adsorbent for selective removal of copper. *Desalination*, *228*, 135–149.

Renault, F., Morin-Crini, N., Gimbert, F., Badot, P. M., & Crini, G. t. (2008). Cationized starch-based material as a new ion-exchanger adsorbent for the removal of C.I. Acid Blue 25 from aqueous solutions. *Bioresource Technology*, *99*, 7573–7586.

Sengil, I., & Özacar, A. M. (2009). Competitive biosorption of Pb^{2+}, Cu^{2+} and Zn^{2+} ions from aqueous solutions onto valonia tannin resin. *Journal of Hazardous Materials*, *166*, 1488–1494.

Sengil, I., Özacar, A., & Türkmenler, M. H. (2009). Kinetic and isotherm studies of Cu(II) biosorption onto valonia tannin resin. *Journal of Hazardous Materials*, *162*, 1046–1052.

Tan, I. A. W., Ahmad, A. L., & Hameed, B. H. (2009). Adsorption isotherms, kinetics, thermodynamics and desorption studies of 2,4,6-trichlorophenol on oil palm empty fruit bunch-based activated carbon. *Journal of Hazardous Materials*, *164*, 473–482.

Tempkin, M. J., & Pyzhev, V. (1940). Kinetics of ammonia synthesis on promoted iron catalysts. *Acta Physicochimica URSS*, *12*, 217–222.

Tseng, J. Y., Chang, C. Y., Chang, C. F., Chen, Y. H., Chang, C. C., Ji, D. R., et al. (2009). Kinetics and equilibrium of desorption removal of copper from magnetic polymer adsorbent. *Journal of Hazardous Materials*, *171*, 370–377.

Wan, H. S. (2008). *Using cyclodextrin to control the branching structure of polymerized products*. D. Shanghai Jiao Tong University., pp. 35–37.
Xie, J. J., Chen, Q., Liu, S., & Xu, Y. (2007). Absorbency properties and reaction-ratio of AM/AA superabsorbent copolymer. *Journal of Central South University of Forestry & Technology*, *27*, 54–59.
Xie, D. M., & Sun, W. X. (2006). Cyclodextrin and polymers supramolecular complexes as biomaterials. *Journal of Materials Science and Engineering*, *24*, 623–626.
Zhao, G. X., Zhang, H. X., Fan, Q. H., Ren, X. M., Li, J. X., Chen, Y. X., et al. (2010). Sorption of copper(II) onto super-adsorbent of bentonite–polyacrylmide composites. *Journal of Hazardous Materials*, *173*, 661–668.